



# Hypoxia-mimetic agents desferrioxamine and cobalt chloride induce leukemic cell apoptosis through different hypoxia-inducible factor-1 $\alpha$ independent mechanisms

M. Guo, L.-P. Song, Y. Jiang, W. Liu, Y. Yu and G.-Q.Chen

Health Science Center, Shanghai Institutes for Biological Sciences and Graduate School of Chinese Academy of Sciences, Shanghai Jiaotong University School of Medicine (SJU-SM, formerly Shanghai Second Medical University), Shanghai 200025, China (M. Guo, L.-P. Song, G.-Q.Chen ); Department of Pathophysiology, Key Laboratory of Cell Differentiation and Apoptosis, SJU-SM, Shanghai 200025, China (Y. Jiang, W. Liu, Y. Yu, G.-Q.Chen )

Published online: 21 December 2005

**Hypoxia presents pro-apoptotic and anti-apoptotic biphasic effects that appear to be dependent upon cell types and conditions around cells. The substantial reports demonstrated that commonly used hypoxia-mimetic agents cobalt chloride (CoCl<sub>2</sub>) and desferrioxamine (DFO) could also induce apoptosis in many different kinds of cells, but the mechanism was poorly understood. In this work, we compare the apoptosis-inducing effects of these two hypoxia-mimetic agents with acute myeloid leukemic cell lines NB4 and U937 as *in vitro* models. The results show that both of them induce these leukemic cells to undergo apoptosis with a loss of mitochondrial transmembrane potentials ( $\Delta\Psi_m$ ), the activation of caspase-3/8 and the cleavage of anti-apoptotic protein Mcl-1, together with the accumulation of hypoxia-inducible factor-1 alpha (HIF-1 $\alpha$ ) protein, a critical regulator for the cellular response to hypoxia. Metavanadate and sodium nitroprusside significantly abrogate DFO rather than CoCl<sub>2</sub>-induced mitochondrial  $\Delta\Psi_m$  collapse, caspase-3/8 activation, Mcl-1 cleavage and apoptosis, but they fail to influence DFO and CoCl<sub>2</sub>-induced HIF-1 $\alpha$  protein accumulation. Moreover, inducible expression of HIF-1 $\alpha$  gene dose not alter DFO and CoCl<sub>2</sub>-induced apoptosis in U937 cells. In conclusion, these results propose that although both DFO and CoCl<sub>2</sub>-induced leukemic cell apoptosis by mitochondrial pathway-dependent and HIF-1 $\alpha$ -independent mechanisms, DFO and CoCl<sub>2</sub>-induced apoptosis involves different initiating signal pathways that remain to be investigated.**

**Keywords:** apoptosis; cobalt chloride; desferrioxamine; HIF-1 $\alpha$ ; leukemia.

## Introduction

Apoptosis, a cell suicide mechanism used by metazoans to eliminate deleterious cells, plays a major role in the proper development of most tissues and is also critical for the maintenance of organ function in the adult.<sup>1</sup> As widely shown, apoptosis can be initiated by many extracellular and intra-

cellular signal molecules or physiological and pathological inducers. During severe hypoxia or anoxia, for instance, the cell initiates apoptosis to prevent the accumulation of cells with hypoxia-induced mutation,<sup>2</sup> presumably because hypoxia induces genetic instability by the induction of fragile sites causing gene amplification<sup>3</sup> and reduces DNA mismatch repair activity due to decreased MLH1 and PMS2 proteins.<sup>4</sup> It appears that many different mechanisms contribute to hypoxia-induced apoptosis. Thereinto, the most direct induction of hypoxia-induced apoptosis is the inhibition of the electron transport chain at the inner membrane of the mitochondria and the generation of radicals, especially reactive oxygen species (ROS). These alterations cause a loss of mitochondrial transmembrane potentials ( $\Delta\Psi_m$ ), the release of cytochrome C into cytosol and ensuring formation of a multimeric protein complex containing Apaf-1, cytochrome C, and caspase-9.<sup>1</sup> In addition, hypoxia-induced c-Jun NH<sub>2</sub>-terminal kinase (JNK) activation was also reported to play a critical role in apoptosis regulation of melanoma cells *in vitro* and *in vivo*,<sup>5</sup> and both mitochondrial and cell death receptor-mediated apoptotic pathways to contribute to hypoxia-induced apoptosis in oral carcinoma cells.<sup>6</sup>

On the other hand, apoptosis was significantly less when staurosporine, a potent apoptotic inducer, was added to hypoxic cells, compared with normoxic ones.<sup>7</sup> Such a resistance to hypoxia-induced apoptosis was proposed to involve multiple factors targeting different stages of apoptosis, at least including hypoxic induction of inhibitor of apoptosis protein-2 (IAP-2) and Bcl-X<sub>L</sub>.<sup>8</sup> Correspondingly, hypoxia, a common feature of solid tumors, was also widely considered to contribute to the resistance of cancer cells to ionizing radiation and chemotherapy-induced apoptosis.<sup>9</sup>

Cobalt chloride (CoCl<sub>2</sub>) and the iron chelator desferrioxamine (DFO) are two commonly used hypoxia-mimetic agents, because like hypoxia, they can block the degradation and thus induce the accumulation of hypoxia-inducible factor-1alpha (HIF-1 $\alpha$ ) protein,<sup>10</sup> a critical regulator for the cellular response to hypoxia.<sup>11</sup> The substantial reports

Correspondence to: G.-Q.Chen, 280, Chong-Qing South Road, Shanghai 200025, China. Tel.: +86-21-64154900; Fax: +86-21-64154900; e-mail: chengq@shsmu.edu.cn or gqchen@sibs.ac.cn

demonstrated that they could induce apoptosis in many different kinds of cells. For examples,  $\text{CoCl}_2$  was shown to induce apoptosis in rat C6 glioma cells,<sup>12</sup> human alveolar macrophages,<sup>13</sup> neuronal PC12 cells<sup>14</sup> and HeLa human cervical cancer cells,<sup>15</sup> although  $\text{CoCl}_2$  reduced the apoptotic death induced by tert-butyl hydroperoxide and serum deprivation in hepatoma cell line HepG<sub>2</sub>.<sup>16</sup> DFO was shown to induce apoptosis in activated T lymphocytes and HL-60 cells, human leukemic cell line CCRF-CEM, Kaposi's sarcoma cells and neuroblastoma cells, and others.<sup>17-23</sup> However, mechanisms of apoptosis mediated by DFO and  $\text{CoCl}_2$  are poorly understood.

Although leukemic cells do not form a well-circumscribed "mass" like solid tumors, oxygen levels in bone marrow (BM) in patients with leukemia may be decreased as a result of fast-growth of leukemic cells, which is possibly further aggravated with anemia commonly developed in newly diagnosed patients. In the matter of fact, low oxygen environment around leukemic cells in BM has been observed in the Brown Norwegian rat that was inoculated by leukemic cells and normal cells.<sup>24</sup> To investigate the effects of hypoxia on leukemic cells, therefore, is necessary. By comparing the apoptosis-inducing effects of hypoxia-mimetic agents  $\text{CoCl}_2$  and DFO on acute myeloid leukemic (AML) cells, in the present work, we showed that both DFO and  $\text{CoCl}_2$  induce leukemic cells apoptosis by mitochondrial pathway-dependent and HIF-1 $\alpha$ -independent mechanisms, but DFO and  $\text{CoCl}_2$ -induced apoptosis involves different initiating signal pathways.

## Materials and methods

### Reagents

$\text{CoCl}_2$ , DFO, sodium metavanadate and sodium nitroprusside (SNP) were purchased from Sigma (St Louis, MO) and dissolved in ultrapure water. Mouse anti-HIF-1 $\alpha$  and mouse anti-caspase-8 monoclonal antibodies were purchased from Becton Dickinson (Palo Alto, CA), mouse monoclonal anti-PARP and rabbit polyclonal anti-Mcl-1 antibodies from Santa Cruz Co (Santa Cruz, CA), rabbit anti-caspase-3 polyclonal antibody from Cell Signaling (Beverly, MA) and mouse anti- $\beta$ -actin monoclonal antibody from EMD Biosciences (San Diego, CA).

### Cell lines and culture

Two leukemic cell lines, NB4 cell line from acute promyelocytic leukemia (a kind gift of Dr. Michel Lannotte, INSERM U-496, Centre G. Hayem, Hospital Saint-Louis, Paris, France) and U937 cell line from acute myelomonocytic leukemia (from Cell Bank of Shanghai Institutes for Biological Sciences, Shanghai, China), were cultured in RPMI-1640 medium (Sigma, St Louis, MO) supplemented with 10%

heat-inactivated fetal calf serum (Gibco BRL, Gaithersburg, MD) in a 5%  $\text{CO}_2$ -95% air humidified atmosphere at 37°C for experiments. Cells were seeded at  $2-5 \times 10^5$  cells/ml and cell viability was determined by the trypan-blue exclusion assay. For the assay of the concentrations of nitric oxide (NO) in the medium, which were performed by Griess Reagent System according to the manufacturer's instruction (Promega, Madison, WI), cells were incubated in phenol red-free RPMI-1640 medium (Gibco BRL, Gaithersburg, MD).

U937T cell line, which constitutionally expresses the tetracycline-controlled transactivator (tTA), is a kind gift of Dr. Grossveld G.<sup>25</sup> To generate the cell line with stable inducible expression of HIF-1 $\alpha$  protein, the BDTM Tet-off gene expression system was used (BD Clontech, Palo Alto, CA). Briefly, HIF-1 $\alpha$  cDNA was ligated to pTRE2hyg (BD Clontech, Palo Alto, CA), generating the tTA responsible expression plasmid pTRE2hyg-HIF-1 $\alpha$ . The plasmid pTRE2hyg-HIF-1 $\alpha$  and empty vector plasmid pTRE2hyg were respectively transfected into U937T cells by electroporation at 0.17 kV and 960  $\mu\text{F}$  on a Bio-Rad gene pulser (Bio-Rad, Hercules, CA), respectively generating U937T<sup>HIF-1 $\alpha$</sup>  and U937T<sup>empty</sup> cells. Both cell lines were selected and maintained by 500  $\mu\text{g}$  of hydromycin B per ml medium in the presence of 0.5  $\mu\text{g}$  of puromycin and 1  $\mu\text{g}$  of tetracycline per ml medium. HIF-1 $\alpha$  expression after tetracycline withdrawal in U937T<sup>HIF-1 $\alpha$</sup>  cells was confirmed by western blot.

### Apoptosis assay

Besides cell morphology with Wright's staining on cytopsin preparations of the cell suspensions, the nuclear DNA content distribution and annexin-V assay were used to assess apoptosis. To assess the distribution of nuclear DNA content, cells were collected, rinsed and fixed overnight in 70% cold ethanol at  $-20^\circ\text{C}$ . Then, cells were treated with Tris-HCl buffer (pH 7.4) supplemented with 1% RNase A and stained with 25  $\mu\text{g}/\text{ml}$  propidium iodide (PI, Sigma, St. Louis, MO). The samples were read on a Coulter Elite Flow Cytometer using Elite software program 4.0 for 2 colors detector (Beckman Coulter, Miami, FL). The percentage of cells in the apoptotic sub-G<sub>1</sub> phase was calculated using multicycle software (Phoenix Flow Systems). For annexin-V assay, cells were incubated with 10  $\mu\text{l}$  PI and 5  $\mu\text{l}$  FITC-annexin-V (BD Biosciences, Franklin Lakes, NJ) at room temperature for 15 min. Then, cells were analyzed on a flow cytometry (Beckman Coulter, Miami, FL). Annexin-V binds to those cells that express phosphatidylserine on the outer layer of the cell membrane, and propidium iodide stains the cellular DNA of those cells with a compromised cell membrane. This allows for the discrimination of live cells (unstained with either fluorochrome) from apoptotic cells (stained only with annexin-V) and necrotic cells (stained with both annexin-V and PI).

### Flow cytometric assays for mitochondrial transmembrane potentials

The mitochondrial  $\Delta\Psi_m$  assay was performed as described previously.<sup>26</sup> Briefly, about  $10^5$  cells were rinsed with PBS and incubated with 10  $\mu\text{g/ml}$  rhodamine 123 (Rh123, Sigma, St. Louis, MO) at 37°C, 30 min. Subsequently, cells were washed with PBS and stained with 25  $\mu\text{g/ml}$  PI. Fluorescent intensities of Rh123 and/or PI were determined by flow cytometry (Beckman Coulter, Miami, FL).

### Semi-quantitative RT-PCR analysis

Total RNAs were extracted from U937 and NB4 cells by TRIzol reagent (Gibco BRL, Gaithersburg, Maryland), and reverse transcriptions were performed by TaKaRa RNA PCR kit (Takara, Dalian, China) following manufacturer's instructions. HIF-1 $\alpha$  cDNA and  $\beta$ -actin cDNA were amplified in the same tube by the following primers: GGA TCC TGG GTA GGA GAT GGA GAT GC (forward) and GCA CTC AAT CAA GAA GTT GC (reverse) for HIF-1 $\alpha$ ; CAT CCT CAC CCT GAA GTA CCC (forward) and AGC CTG GAT AGC AAC GTA CAT G (reverse) for  $\beta$ -actin cDNA. PCR amplification was performed for 26 cycles with denaturing at 94°C for 30 s, annealing at 58°C for 45 s, and extension at 72°C for 60s using a GeneAmp PCR System 9600 (Perkin-Elmer Norwalk, USA). The signal intensities of amplified HIF-1 $\alpha$  and  $\beta$ -actin fragments were measured by a densitometer. The ratio of signal intensities of HIF-1 $\alpha$  against that of  $\beta$ -actin in the same amplified tube represents the relative level of HIF-1 $\alpha$  mRNA. All RT-PCR reactions were repeated at least 3 times.

### Western blots

Cells were dissolved in lysis buffer (100mM Tris-HCl, pH6.8, 4% SDS, 20% glycerin, 200mM dithiothreitol) and relatively quantified for proteins by DC protein assay kit II (Bio-Rad, Hercules, CA). Equal amount (20–50  $\mu\text{g}$ ) of protein extracts were loaded to 10% SDS-PAGE gel and transferred to a nitrocellulose membrane. Equal loading amounts of proteins were further ensured by the stain of Ponceau S on the membrane. The membrane was sequentially blocked in 5% fat-free milk and then incubated with the indicating antibodies, followed by HRP-linked secondary antibodies in a 5% fat-free milk solution. Detection was performed by chemiluminescence phototope-HRP kit according to manufacturer's instructions (Amersham, Buckinghamshire, UK). All blots were stripped and re-probed with anti- $\beta$ -actin.

### Statistical analysis

The two-sided Student's-test was used to compare the difference between untreated and treated cells.  $p < 0.05$  was considered to be statistically significant.

## Results

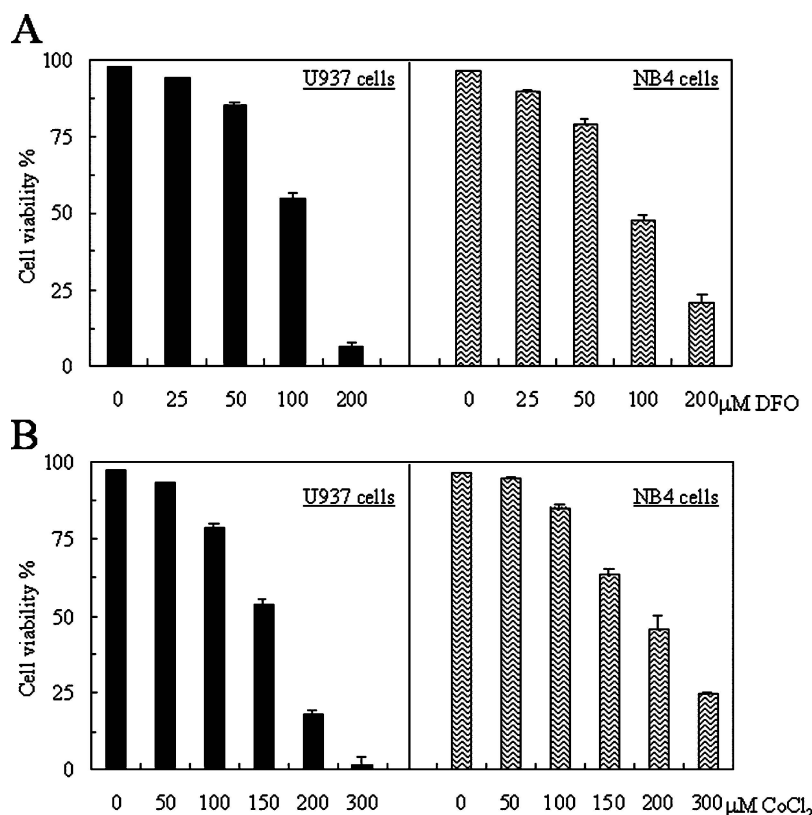
### Desferrioxamine and cobalt chloride at higher concentrations induce leukemic cell apoptosis

As we showed previously,<sup>27,28</sup> lower concentrations of DFO (equal to and less than 25  $\mu\text{M}$ ) and  $\text{CoCl}_2$  (equal to and less than 50  $\mu\text{M}$ ) did not significantly reduce cell viability of leukemic NB4 and U937 cells. At higher concentrations, however, they induced these two cells to die in a dose-dependent manner, as evidenced by the detection of cell viability (Figure 1). When treated by 100  $\mu\text{M}$  of DFO or 200  $\mu\text{M}$  of  $\text{CoCl}_2$  for 24 h, furthermore, NB4 cells presented profound morphological features of apoptotic cells, such as cell shrinking, chromatin condense and nuclear fragmentation with intact cell membrane (Figure 2A). These cells also presented annexin-V<sup>+</sup> with PI<sup>-</sup> staining and time-dependent increase of hypoploid cells (also called sub-G<sub>1</sub> cells) on flow cytometry (Figure 2B, C), two sensitive and specific indications of apoptotic cells in suspension culture.<sup>29,30</sup> Of note, some secondary necrotic cells, as indicated by double positive annexin-V/PI staining, could also be seen (Figure 2B). Similar results could also be obtained in DFO (100  $\mu\text{M}$ ) and  $\text{CoCl}_2$  (200  $\mu\text{M}$ )-treated U937 cells (data not shown). In total, these results support that higher concentrations of DFO and  $\text{CoCl}_2$  induce cell death by way of apoptosis in leukemic cells.

### Desferrioxamine and cobalt chloride-induced apoptosis involves a loss of mitochondria transmembrane potentials, caspase-3/8 activation and Mcl-1 cleavage

It has been well known that a complex cellular signaling network contributes to the regulation of apoptosis. In most cases, a central player in the execution of apoptosis is aspartic acid-directed cysteine proteases called caspases, which can be activated by the cell surface death receptor pathway and the mitochondria-initiated pathway.<sup>31</sup> To determine whether DFO and  $\text{CoCl}_2$  can damage mitochondria  $\Delta\Psi_m$ , NB4 and U937 cells were stained with PI and Rh123, latter being a lipophilic cation that is taken up by mitochondria in proportion to the  $\Delta\Psi_m$ .<sup>26</sup> As depicted in Figure 3A, both DFO and  $\text{CoCl}_2$  induced low Rh123 staining with or without PI-positive staining, indicating that these two agents induced mitochondrial  $\Delta\Psi_m$  collapse. In parallel to this, DFO and  $\text{CoCl}_2$  also activated caspase-3, which was measured by western blot with specific anti-active caspase-3 antibody. Notably, these two agents also induced cleaved activation of caspase-8, that presented as two fragments respectively with 40 kD and 23 kD.<sup>32</sup> PARP, a specific substrate of caspase-3, was also degraded (Figure 3B). It was worthy noting that  $\text{CoCl}_2$  and especially DFO also reduced Mcl-1 protein, an anti-apoptotic member of Bcl-2 family, with appearance of a fragment of 25 kD (Figure 3C).

**Figure 1.** Higher concentrations of either desferrioxamine or cobalt chloride reduce cell viability of NB4 and U937 cells. U937 (left) and NB4 cells (right) were treated with indicated concentrations ( $\mu\text{M}$ ) of DFO (A) and  $\text{CoCl}_2$  (B) for 24 h. Cell viability was measured by trypan-blue exclusion assay. Every column represented the mean with bar as *sd* of triplicates in an independent experiment. All experiments were repeated three times with the similar results.



### Metavanadate antagonizes desferrioxamine-induced apoptosis of leukemic cells without the decrease of HIF-1 $\alpha$ protein

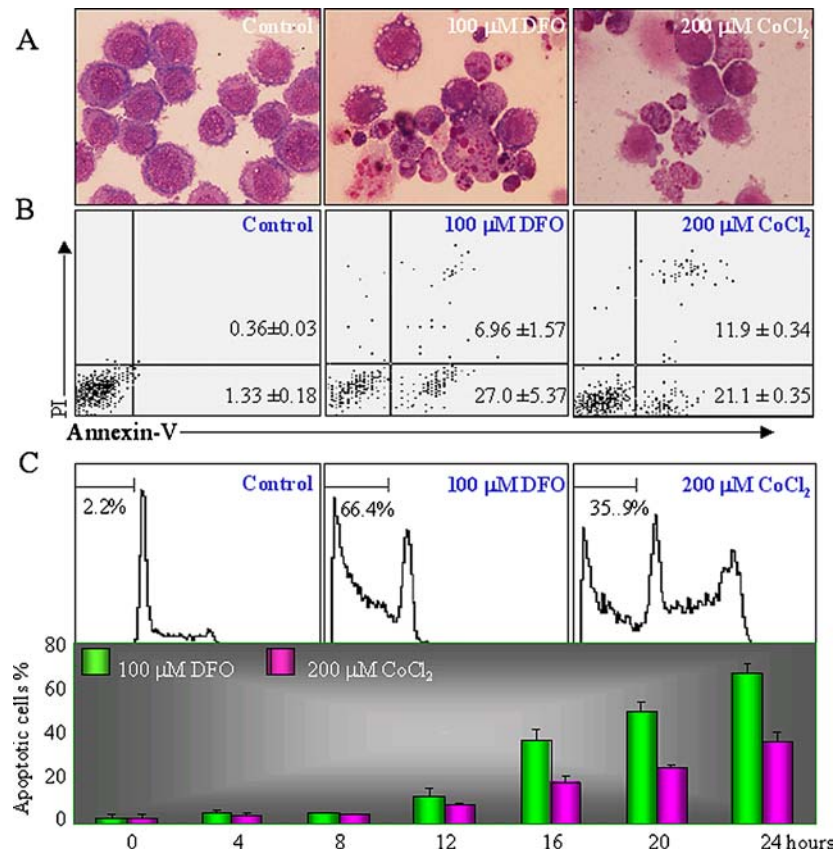
To elucidate whether HIF-1 $\alpha$  protein has something to do with DFO and  $\text{CoCl}_2$ -induced apoptosis, we tried to use some agents to interfere with HIF-1 $\alpha$  expression. According to a report that vanadate induced the expression of HIF-1 $\alpha$  in DU145 human prostate carcinoma cells,<sup>33</sup> we treated leukemic cells with DFO or  $\text{CoCl}_2$  plus metavanadate. We showed that 20  $\mu\text{M}$  metavanadate alone had no effect on HIF-1 $\alpha$  expression (Figure 4A). It also failed to affect HIF-1 $\alpha$  protein level in the presence of apoptosis-inducing concentration of DFO and  $\text{CoCl}_2$  (Figure 4B). It should be pointed out that due to the contrast with that found in DU145 cells,<sup>33</sup> we repeated this experiment for 5 times with the same results. In spite of this, we still investigated the possible effects of metavanadate on DFO-induced apoptosis. For this set of experiments, NB4 cells were co-treated with 100  $\mu\text{M}$  of DFO and different concentrations ( $\mu\text{M}$ ) of metavanadate for 24 h. As can be seen in Figure 5A, 5–20  $\mu\text{M}$  of metavanadate treatment alone had no effects on cell viability, mitochondrial  $\Delta\Psi_m$  and annexin-V staining.

More surprisingly, metavanadate significantly blocked DFO-induced mitochondrial  $\Delta\Psi_m$  collapse and apoptosis in a concentration-dependent manner. As consistent with this, metavanadate also inhibited DFO-induced caspase-3 activation and the cleavage of PARP (Figure 5B) and Mcl-1 (Figure 3C).

### Sodium nitroprusside also antagonizes DFO-induced apoptosis rather than the accumulation of HIF-1 $\alpha$ protein in leukemic cells

It has been well known that vanadate exerts a wide-spectrum effects on cells, one of which is to potently activate NO synthase and thus to induce NO production.<sup>34</sup> Although metavanadate did not induce the production of NO in our tests (Figure 5C), we still explored the potential effects of another commonly-used NO donor sodium nitroprusside (SNP), which significantly increased the production of NO (Figure 5C), on DFO-induced apoptosis in NB4 and U937 cells. Like those seen in metavanadate treatment, 100  $\mu\text{M}$  of SNP affected neither the transcription of HIF-1 $\alpha$  nor DFO-induced HIF-1 $\alpha$  protein accumulation (Figure 4), but it

**Figure 2.** Higher concentrations of desferrioxamine and cobalt chloride induce apoptosis in leukemic cells (**A** and **B**). NB4 cells were treated with or without 100  $\mu\text{M}$  of DFO and 200  $\mu\text{M}$  of  $\text{CoCl}_2$  for 24 h. Cell morphology (**A**) was observed under microscope (magnificent,  $\times 1000$ ) and annexin-V<sup>+</sup> cells (**B**) were detected on flow cytometry as described in 'Materials and Methods'. The percentages of annexin-V<sup>+</sup>/PI<sup>-</sup> and annexin-V<sup>+</sup>/PI<sup>+</sup> cells were shown in the corresponding quadrants as mean  $\pm$  sd of triplicates of a separate experiment. (**C**). NB4 cells were treated with or without 100  $\mu\text{M}$  of DFO and 200  $\mu\text{M}$  of  $\text{CoCl}_2$  for h as indicated. The representative histograms showing contribution of nuclear DNA content were shown (top panels) and the percentages of sub-G<sub>1</sub> cells were given with mean  $\pm$  sd of triplicates in an independent experiment. The similar results were also gotten in U937 cells (data not shown). All experiments were repeated three times with similar results.



significantly abrogated DFO-induced mitochondrial  $\Delta\Psi_m$  (Figure 6A) and the percentages of annexin-V<sup>+</sup> cells (Figure 6B) and sub-G<sub>1</sub> cells (Figure 6C) as well as caspase-3 activation, PARP cleavage (Figure 5B) and Mcl-1 cleavage (Figure 3C).

### Metavanadate and sodium nitroprusside fail to antagonize $\text{CoCl}_2$ -induced apoptosis of leukemic cells

In the next phase of analysis, we observed effects of metavanadate and SNP on the action of apoptosis-inducing concentration (200  $\mu\text{M}$ ) of  $\text{CoCl}_2$  in NB4 and U937 cells. The results showed that neither metavanadate nor SNP affected  $\text{CoCl}_2$ -induced HIF-1 $\alpha$  protein accumulation (Figure 4). Unlike their effects on DFO, more unexpectedly, these agents failed to reduce  $\text{CoCl}_2$ -induced apoptosis, caspase-3 activation, PARP cleavage (Figure 7) and Mcl-1 cleavage (Figure 3C).

### Inducible expression of HIF-1 $\alpha$ has no effect on DFO and $\text{CoCl}_2$ -induced apoptosis

To further elucidate whether HIF-1 $\alpha$  contributes to DFO and  $\text{CoCl}_2$ -induced apoptosis, we generated a HIF-1 $\alpha$  inducible expressing cell line called U937T<sup>HIF-1 $\alpha$</sup>  with U937T<sup>empty</sup> and their parental U937T cell as controls, as described in "Materials and Methods". As can be seen in Figure 8A, HIF-1 $\alpha$  mRNA and protein levels were significantly induced after tetracycline withdrawal.  $\text{CoCl}_2$  and DFO further elevated HIF-1 $\alpha$  protein in U937T<sup>HIF-1 $\alpha$</sup>  cells to a greater degree than that in U937T<sup>empty</sup> cells (Figure 8B). To our surprise, DFO at 100  $\mu\text{M}$  and  $\text{CoCl}_2$  at 200  $\mu\text{M}$  failed to induce U937T cells to apoptose (Figure 8C). We speculated that the transfection of tetracycline-controlled transactivator interfered the context of U937T cells with unknown reasons. Thus, we used the higher concentrations of DFO and  $\text{CoCl}_2$  to treat U937T<sup>empty</sup> and U937T<sup>HIF-1 $\alpha$</sup>  cells. As shown in Figure 8D, highly expressed HIF-1 $\alpha$  did not modulate these concentrations of DFO and  $\text{CoCl}_2$ -induced apoptosis in U937T<sup>HIF-1 $\alpha$</sup>

**Figure 3.** DFO and CoCl<sub>2</sub> induce mitochondrial transmembrane potential loss and caspase-3/8 activation and Mcl-1 cleavage in NB4 and U937 cells. **(A and B).** NB4 and U937 cells were treated with or without 100 μM of DFO and 200 μM of CoCl<sub>2</sub> for 24 h. Then, the mitochondrial ΔΨ<sub>m</sub> was measured on flow cytometry **(A)** top, NB4; bottom, U937 cells and caspase-3, caspase-8 and PARP proteins were detected by western blots **(B)**. Δ represents their cleaved fragments. Values in A represent the mean ± sd of Rh123<sup>low</sup>/PI<sup>-</sup> and Rh123<sup>low</sup>/PI<sup>+</sup> cells % of triplicates in an independent experiment. All tests were repeated up to three times with similar results. **(C)** NB4 and U937 cells were treated with 100 μM of DFO or 200 μM of CoCl<sub>2</sub> with and without vanadate (20 μM) or SNP (100 μM) for 24 h, Mcl-1 protein was detected by western blots. Δ represents its cleaved 25 kD fragment.

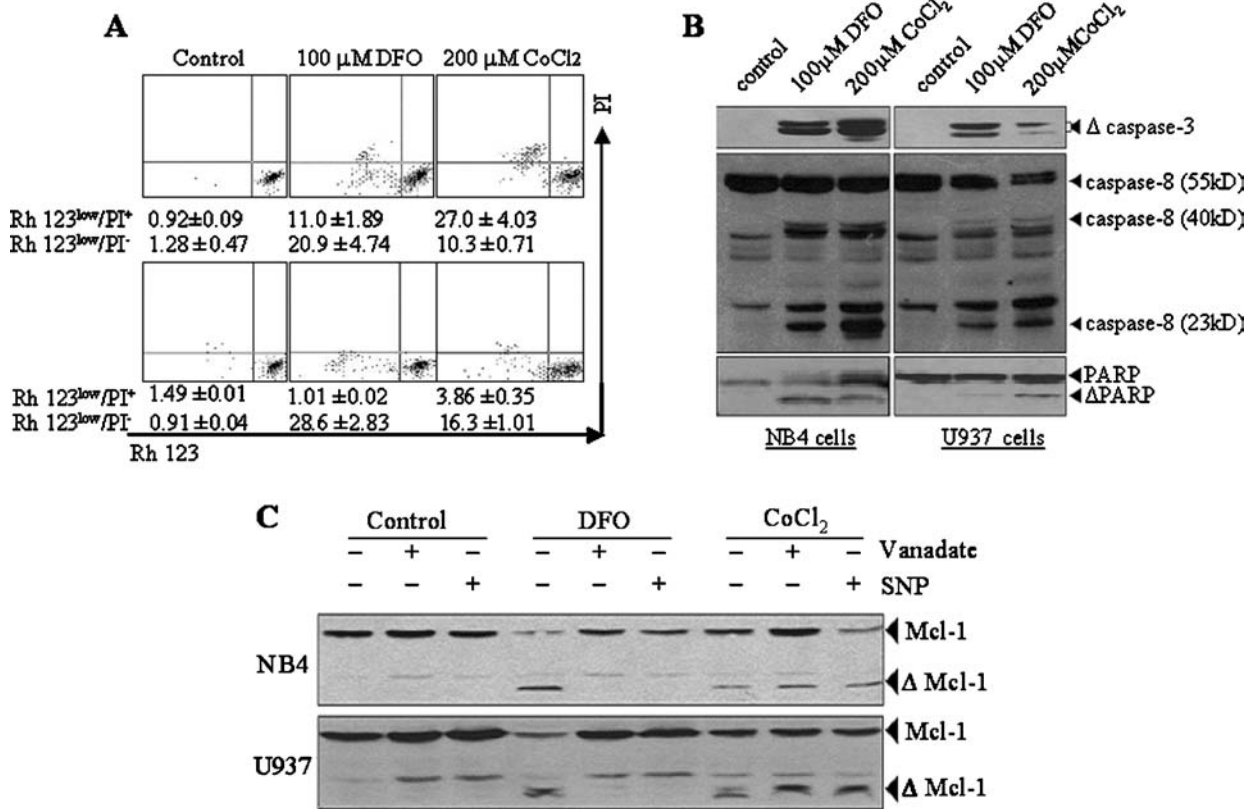


**Figure 4.** Effects of metavanadate or SNP and apoptosis-inducing concentrations of DFO/CoCl<sub>2</sub> on the mRNA and protein levels of HIF-1α. NB4 and U937 cells were treated with 100 μM of DFO or 200 μM of CoCl<sub>2</sub> with and without metavanadate (20 μM) or SNP (100 μM) for 24 h. **(A)** Semi-quantitative RT-PCR for HIF-1α mRNA were performed as described in “Materials and Methods”. Lower panels represent the ratio of HIF-1α/β-actin mRNA under the indicated treatments. **(B)** HIF-1α proteins were analyzed by western blots with β-actin as equal loading control. Independent experiments were repeated three times and the fluctuation of results was minimal.

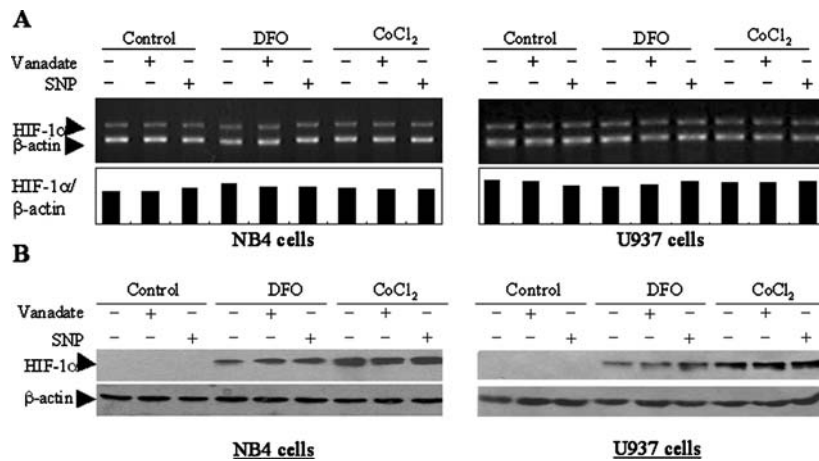


**Figure 5.** Metavanadate mitigates DFO-induced apoptosis in U937 cell in a concentration-dependent manner. U937 cells were treated with various concentrations of metavanadate and/or 100  $\mu$ M of DFO for 24 h. (A) Cell viability (top), annexin-V (middle) and mitochondrial  $\Delta\Psi_m$  (bottom) were measured as described above. Every column and bar represented the mean and *sd* (compared with DFO-treated group, \**p* < 0.05; # *p* < 0.01). (B) The active ( $\Delta$ ) caspase-3 and PARP proteins were detected by Western blot with  $\beta$ -actin as equally loading control. All tests were repeated up to three times with similar results. (C) NB4 and U937 cells were incubated in the phenol red-free medium with 20  $\mu$ M of metavanadate or 100  $\mu$ M of SNP for 24 h, and NO contents in the medium were detected. The values represent mean  $\pm$  *sd* of triplicate samples in an independent experiment.

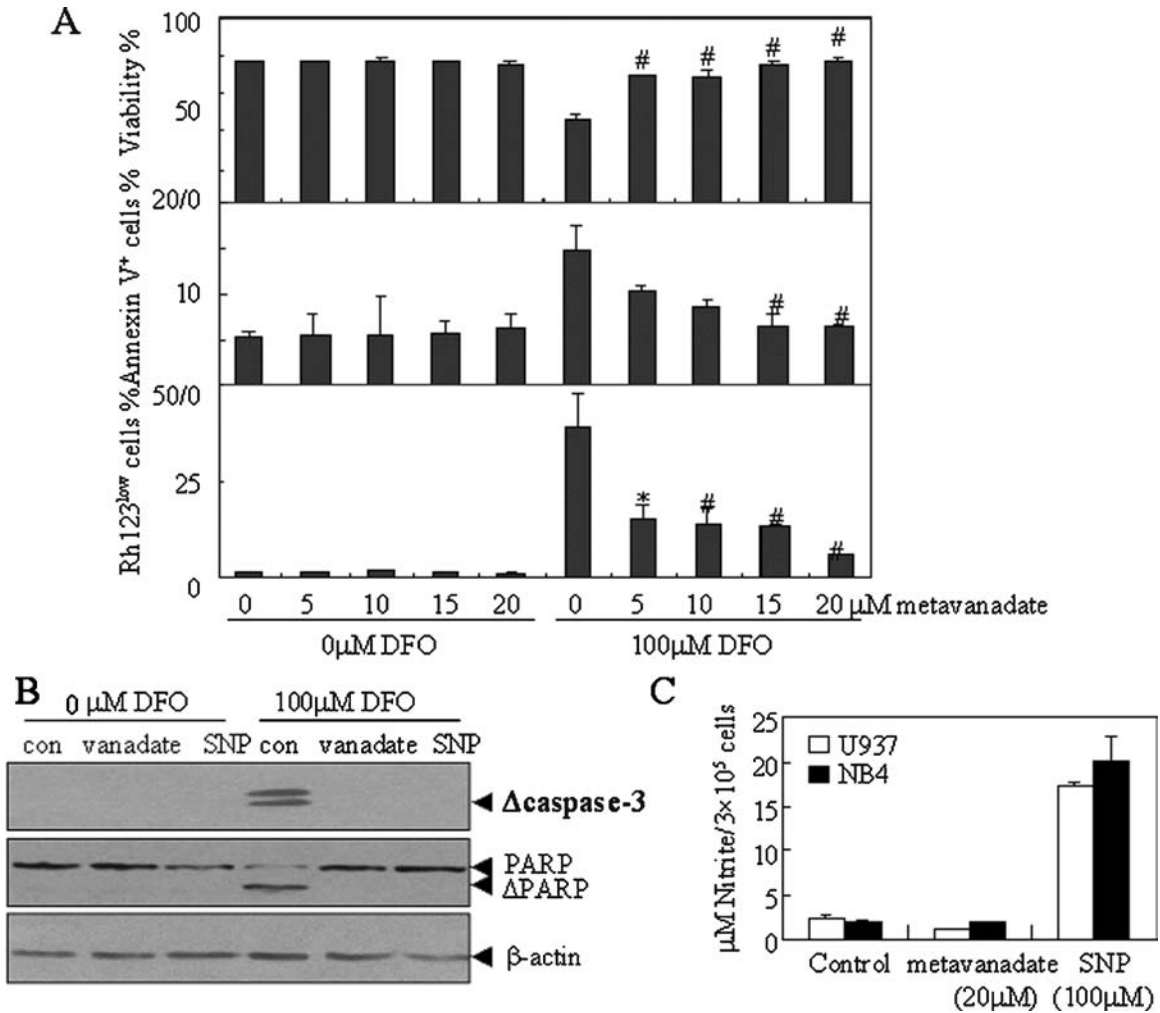


**Figure 6.** SNP mitigates DFO-induced apoptosis in leukemic cells. NB4 cell was treated with 100  $\mu$ M of DFO or/and 100  $\mu$ M of SNP for 24 h. Annexin-V<sup>+</sup> cells (A), the mitochondrial  $\Delta\Psi_m$  (B) and the apoptotic sub-G<sub>1</sub> cells % (C) were measured by flow cytometer. Values in B represent the mean  $\pm$  *sd* of annexin V<sup>+</sup>/PI<sup>-</sup> and annexin V<sup>+</sup>/PI<sup>+</sup> cells of triplicates in an independent experiment.

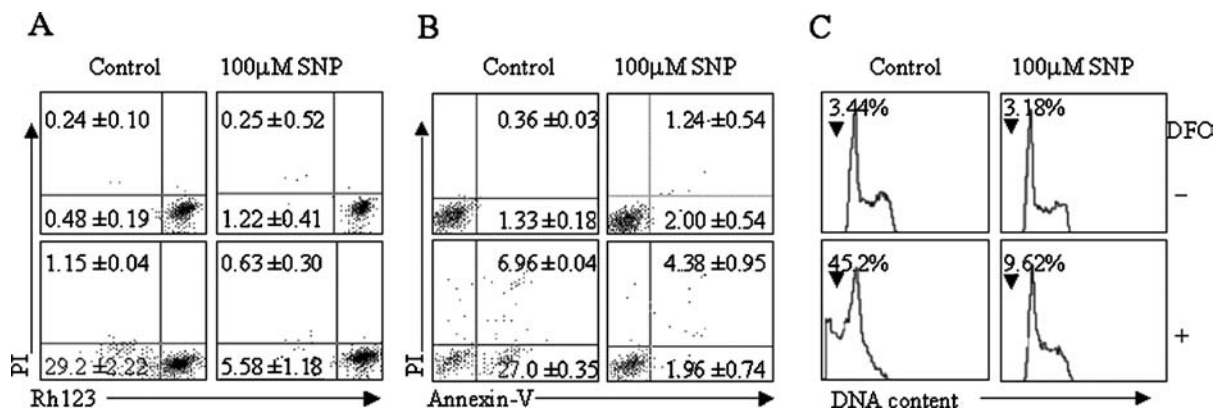
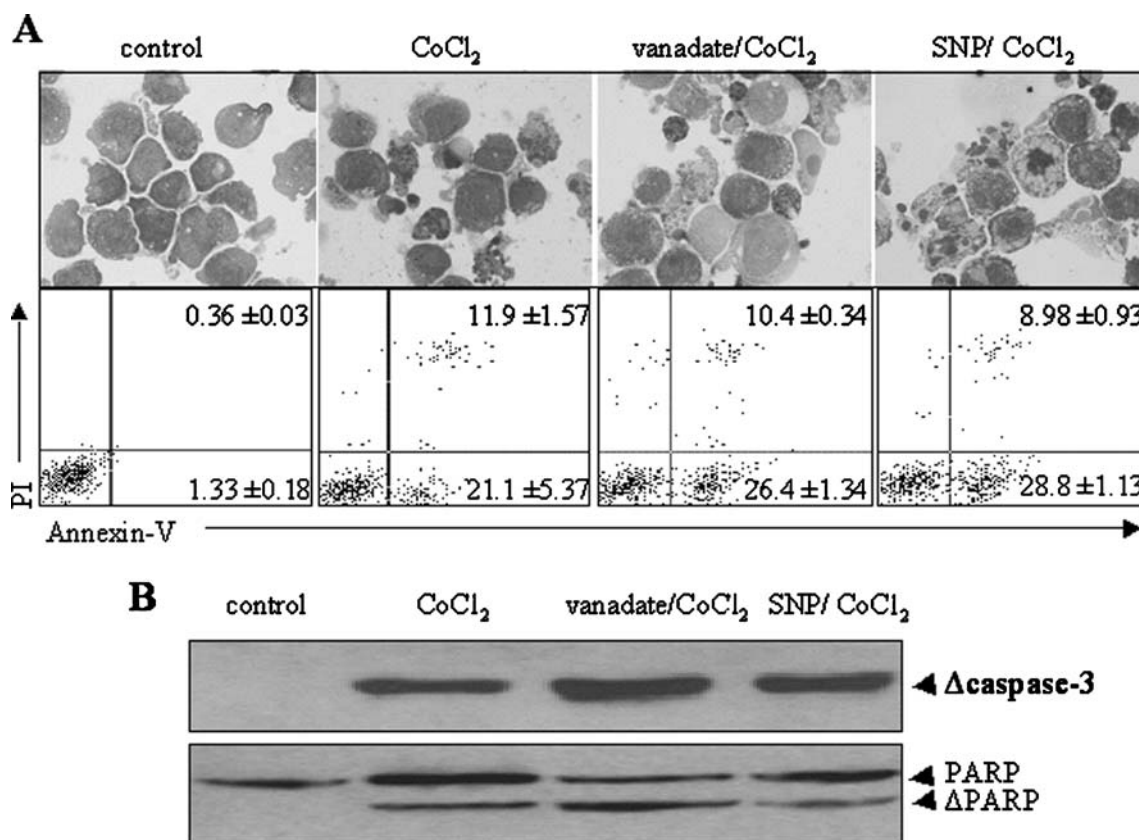


**Figure 7.** Metavanadate and SNP fail to interfere with CoCl<sub>2</sub>-induced apoptosis. U937 cell was treated with 200 μM of CoCl<sub>2</sub> or/and 20 μM of metavanadate or 100 μM of SNP for 24 h. (A) Cells were collected onto slides by cytospin, stained by Wright's staining and observed under microscope (magnificent, ×1000) (top) and cell death was quantified by annexin-V/PI assay on flow cytometry (bottom). Values represent the mean ± sd of annexin V<sup>+</sup>/PI<sup>-</sup> and annexin V<sup>+</sup>/PI<sup>+</sup> cells of triplicates in an independent experiment. (B) The active (Δ) caspase-3 and PARP proteins were detected by western blot.



cell, compared with that in U937T<sup>empty</sup> control cells.

## Discussion

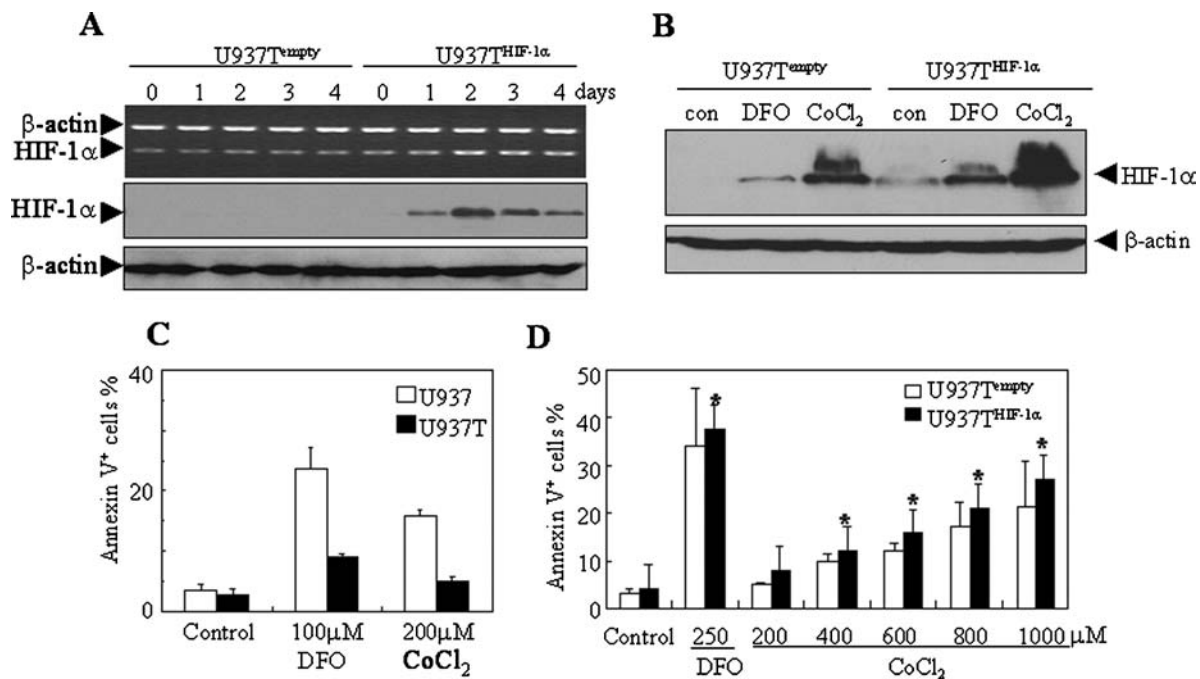
Iron homeostasis is crucial to normal cell metabolism, and its deficiency or excess is associated with numerous disease states. As documented, iron is one of well-known carcinogens or cofactors involved in the pathogenesis of many kinds of cancers in animals, such as adenocarcinomas, colorectal tumors, hepatomas, mammary tumors, mesotheliomas, renal tubular cell carcinomas, and sarcomas.<sup>35</sup> Patients who suffer from hemochromatosis characterized by increased iron absorption and moderate elevation of body iron levels presented the markedly enhanced susceptibility to various malignancies.<sup>36,37</sup> Although the pathogenic role of iron in cancer development and/or progression remains greatly unknown, iron chelators possess considerable anti-tumor activity *in vitro*, *in vivo* and in clinical trials in the treatment of neuroblastoma, leukemia, bladder carcinoma, and hepatocellular carcinoma and so on.<sup>38,39</sup> In the current work, we also showed that greater than 25 μM

of DFO could effectively induce NB4 and U937 leukemic cells to undergo apoptosis by inducing the mitochondrial ΔΨ<sub>m</sub> collapse and caspase-3 activation. Considering that DFO also presents its hypoxia-mimetic effect by stabilizing HIF-1α protein,<sup>40</sup> we extended to investigate the effect of another hypoxia-mimetic agent CoCl<sub>2</sub> on these two leukemic cells. The results showed that CoCl<sub>2</sub> at the concentration of greater than 50 μM also induced these cells to undergo apoptosis via mitochondria pathway-mediated caspase-3 activation. Moreover, DFO and CoCl<sub>2</sub>-induced apoptosis accompanied the cleavage of Mcl-1, supporting recent report from Weng *et al.*,<sup>41</sup> who showed that tumor necrosis factor-related apoptosis-inducing ligand (TRAIL)-induced apoptosis in Jurkat T cells required the specific cleavage of Mcl-1 by caspase-3 and the C-terminal domain of Mcl-1 became proapoptotic as a result of caspase-3 cleavage. Additionally, either DFO or CoCl<sub>2</sub> also activated caspase-8 with apoptosis induction, suggesting the possible role of cell death receptor-mediated apoptotic pathways, like in hypoxia-induced apoptosis in oral carcinoma cell lines.<sup>6</sup>

HIF-1, a heterodimer composed of the rate limiting factor HIF-1α and the constitutively expressed HIF-1β/aryl



**Figure 8.** Inducible expression of HIF-1 $\alpha$  dose not affect DFO and CoCl<sub>2</sub>-induced apoptosis. **(A)** After the withdrawal of tetracycline for the indicated days in U937T<sup>empty</sup> and U937T<sup>HIF-1 $\alpha$</sup>  cells, HIF-1 $\alpha$  mRNA (top) and protein (bottom) were detected by semi-quantitative RT-PCR and western blots. Of note, the primers for  $\beta$ -actin amplification in this experiment was 5'-AGCGGGAAATCGTGC GTGAC-3' (forward) and 5'-TGCTGTCACCTTCACCGTTCC-3' (reverse), which amplified a 684 bp fragment of  $\beta$ -actin. **(B)** After the withdrawal of tetracycline for 24 h, U937T<sup>empty</sup> and U937T<sup>HIF-1 $\alpha$</sup>  cells were treated with 250  $\mu$ M of DFO and 1000  $\mu$ M of CoCl<sub>2</sub> for 24 h, and HIF-1 $\alpha$  proteins were analyzed by western blots with  $\beta$ -actin as equal loading control. **(C)** U937 and U937T cells were treated with or without 100  $\mu$ M of DFO and 200  $\mu$ M of CoCl<sub>2</sub> for 24 h. Annexin-V<sup>+</sup> cells were detected on flow cytometry. Every column and bar represent the mean and *sd* of triplicate samples in an independent experiments out of three repeated ones. **(D)** After the withdrawal of tetracycline for 24 h, U937T<sup>empty</sup> and U937T<sup>HIF-1 $\alpha$</sup>  cells were treated with 250  $\mu$ M of DFO and indicated concentrations ( $\mu$ M) of CoCl<sub>2</sub> for 24 h. Apoptotic cells were measured by annexin-V assay on flow cytometry. Every column represents the mean and *sd* of all three independent experiments with triplicate samples each. \* *p* > 0.05, compared between U937T<sup>empty</sup> and U937T<sup>HIF-1 $\alpha$</sup>  cells under the same treatment.



hydrocarbon receptor nuclear translocator, involves in embryonic development, tumor growth, metastasis, apoptosis and leukemic cell differentiation.<sup>12,42,43</sup> This transcription factor is also involved in apoptosis in the presence of different environmental factors possibly via increasing the stability of wild-type tumor suppressor protein p53 by the direct binding to the p53 ubiquitin ligase MDM2 and even by the direct binding of p53 to the ODD (For oxygen dependent degradation) domain of HIF-1 $\alpha$ , and inducing the expression of the proapoptotic proteins BNIP3 (Bcl2/adenovirus E1B 19 kDa interacting protein 3) and NIX, a BNIP3 homologue, as reviewed by Greijer *et al.*<sup>44</sup> On the other hand, HIF-1 $\alpha$  dimerized with HIF-1 $\beta$  can protect cells from apoptosis induced by several factors.<sup>45</sup> Here, we showed that both DFO and CoCl<sub>2</sub> induced the accumulation of HIF-1 $\alpha$  protein. Previously, it was showed that vanadate induced the expression of HIF-1 $\alpha$  in DU145 human prostate carcinoma cells.<sup>31</sup> On the contrary, we showed recently that the influence of metavanadate on DFO-induced accumulation and transcriptional activity of HIF-1 $\alpha$  protein was dependent upon the concentrations of DFO and metavanadate in leukemic cells and COS-7 cells.<sup>46</sup> Lower concentration of metavanadate almost completely blocked non-toxic con-

centration (10  $\mu$ M) but not higher concentrations of DFO-induced accumulation of HIF-1 $\alpha$  protein. In agreement with this, here we showed that 20  $\mu$ M metavanadate failed to reduce HIF-1 $\alpha$  protein in the presence of apoptosis-inducing concentrations of DFO and CoCl<sub>2</sub>. These results indicate the complication of the effect of metavanadate on HIF-1 $\alpha$ , which possibly depends on cell context besides the concentration ratio of metavanadate against DFO. Even so, the most important is that 20  $\mu$ M metavanadate blocked DFO but not CoCl<sub>2</sub>-induced apoptosis, indicating that these two agents-induced apoptosis involves different initiating mechanisms. Combined with the fact that highly expressed HIF-1 $\alpha$  did not increase or decrease DFO and CoCl<sub>2</sub>-induced apoptosis, these data also support that DFO and CoCl<sub>2</sub>-induced apoptosis is HIF-1 $\alpha$ -independent.

Nitric oxide, synthesized from L-arginine by NO synthases, is a small, diffusible, highly reactive molecule with dichotomous regulatory roles under physiological and pathological conditions. As reviewed,<sup>47,48</sup> NO exhibits a double-edged role in apoptosis induction, that is, pro- and anti-apoptotic effects, which is speculated to be dependent on concentration of NO, in which the proapoptotic effect appears to be linked to pathophysiological conditions with

the production of high concentration of NO by the inducible nitric oxide synthase, while anti-apoptotic effect is mainly mediated by low amounts of NO or stimulation of the constitutive, endothelial nitric oxide synthase.<sup>49–51</sup> Metavanadate was reported to potentially activate NO synthase and thus induced NO production.<sup>34</sup> Of note, we could not show that 20  $\mu$ M of metavanadate induced the production of NO, possibly due to low sensitivity of our measured method. However, the commonly used NO donor, SNP, did ameliorate DFO-induced apoptosis but not CoCl<sub>2</sub>-induced apoptosis, indicating that NO-related signal pathway at least partially contributes to DFO but not CoCl<sub>2</sub>-induced apoptosis.

In summary, our results showed that both DFO and CoCl<sub>2</sub> induce leukemic cells to undergo apoptosis by HIF-1 $\alpha$ -independent mechanisms, but they use different initiating mechanisms, in which NO-related signal pathway involves DFO-induced apoptosis.

### Acknowledgments

This work was supported in part by National Key Program for Basic Research of China (NO2002CB512806), National Natural Science Foundation of China (90408009), International Collaborative Items of Ministry of Science and Technology of China (2003DF000038), Grants from Science and Technology Committee of Shanghai (03XD14016; 04DZ14901).

### References

1. Hajra KM, Liu JR. Apoptosome dysfunction in human cancer. *Apoptosis* 2004; 9: 691–704.
2. Reynolds TY, Rockwell S, Glazer PM. Genetic instability induced by the tumor microenvironment. *Cancer Res* 1996; 56: 5754–5757.
3. Coquelle A, Toledo F, Stern S, Bieth A, Debatisse M. A new role for hypoxia in tumor progression: induction of fragile site triggering genomic rearrangements and formation of complex DMs and HSRs. *Mol Cell* 1998; 2: 259–265.
4. Perou CM, Sorlie T, Eisen MB, et al. Molecular portraits of human breast tumours. *Nature* 2000; 406: 747–752.
5. Kunz M, Ibrahim S, Koczan D, et al. Activation of c-Jun NH2-terminal kinase/stress-activated protein kinase (JNK/SAPK) is critical for hypoxia-induced apoptosis of human malignant melanoma. *Cell Growth Differ* 2001; 12: 137–145.
6. Nagaraj NS, Vigneswaran N, Zacharias W. Hypoxia-mediated apoptosis in oral carcinoma cells occurs via two independent pathways. *Mol Cancer* 2004; 3: 38.
7. Dong Z, Wang JZ, Yu F, Venkatachalam MA. Apoptosis-resistance of hypoxic cells: Multiple factors involved and a role for IAP-2. *Am J Pathol* 2003; 163: 663–671.
8. Dong Z, Wang J. Hypoxia selection of death-resistant cells: A role for Bcl-XL. *J Biol Chem* 2004; 279: 9215–9221.
9. Harrison L, Blackwell K. Hypoxia and anemia: Factors in decreased sensitivity to radiation therapy and chemotherapy? *Oncologist* 2004; 9: 31–40.
10. An WG, Kanekal M, Simon MC, Maltepe E, Blagosklonny MV, Neckers LM. Stabilization of wild-type p53 by hypoxia-inducible factor 1  $\alpha$ . *Nature* 1998; 392: 405–408.

11. Semenza GL. Hypoxia-inducible factor 1: master regulator of O<sub>2</sub> homeostasis. *Curr Opin Genet Dev* 1998; 8: 588–594.
12. Yang SJ, Pyen J, Lee I, Lee H, Kim Y, Kim T. Cobalt chloride-induced apoptosis and extracellular signal-regulated protein kinase 1/2 activation in rat C6 glioma cells. *J Biochem Mol Biol* 2004; 37: 480–486.
13. Araya J, Maruyama M, Inoue A, et al. Inhibition of proteasome activity is involved in cobalt-induced apoptosis of human alveolar macrophages. *Am J Physiol Lung Cell Mol Physiol* 2002; 283: L849–L858.
14. Zou W, Yan M, Xu W, et al. Cobalt chloride induces PC12 cells apoptosis through reactive oxygen species and accompanied by AP-1 activation. *J Neurosci Res* 2001; 64: 646–653.
15. Kim HJ, Yang SJ, Kim YS, Kim TU. Cobalt chloride-induced apoptosis and extracellular signal-regulated protein kinase activation in human cervical cancer HeLa cells. *J Biochem Mol Biol* 2003; 36: 468–474.
16. Piret JP, Mottet D, Raes M, Michiels C. CoCl<sub>2</sub>, a chemical inducer of hypoxia-inducible factor-1, and hypoxia reduce apoptotic cell death in hepatoma cell line HepG2. *Ann NY Acad Sci* 2002; 973: 443–447.
17. Becton DL, Roberts B. Antileukemic effects of deferoxamine on human myeloid leukemia cell lines. *Cancer Res* 1989; 49: 4809–4812.
18. Hileti D, Panayiotidis P, Hoffbrand AV. Iron chelators induce apoptosis in proliferating cells. *Br J Haematol* 1995; 89: 181–187.
19. Haq RU, Wereley JP, Chitambar CR. Induction of apoptosis by iron deprivation in human leukemic CCRF-CEM cells. *Exp Hematol* 1995; 23: 428–432.
20. Kovar J, Stunz LL, Stewart BC, Kriegerbeckova K, Ashman RF, Kemp JD. Direct evidence that iron deprivation induces apoptosis in murine lymphoma 38C13. *Pathobiology* 1997; 65: 61–68.
21. Fukuchi K, Tomoyasu S, Tsuruoka N, Gomi K. Iron deprivation-induced apoptosis in HL-60 cells. *FEBS Lett* 1994; 350: 139–142.
22. Simonart T, Degraef C, Andrei G, et al. Iron chelators inhibit the growth and induce the apoptosis of Kaposi's sarcoma cells and of their putative endothelial precursors. *J Invest Dermatol* 2000; 115: 893–900.
23. Fan L, Iyer J, Zhu S, et al. Inhibition of N-myc expression and induction of apoptosis by iron chelation in human neuroblastoma cells. *Cancer Research* 2001; 61: 1073–1079.
24. Jensen PO, Mortensen BT, Hodgkiss RJ, et al. Increased cellular hypoxia and reduced proliferation of both normal and leukaemic cells during progression of acute myeloid leukemia in rats. *Cell Prolif* 2000; 33: 381–395.
25. Boer J, Bonten-Surtel J, Grosveld G. Overexpression of the nucleoporin CAN/NUP214 induces growth arrest, nucleocytoplasmic transport defects, and apoptosis. *Mol Cell Biol* 1998; 18: 1236–1247.
26. Zhu XH, Shen YL, Jing YK, et al. Apoptosis and growth inhibition in malignant lymphocytes after treatment with arsenic trioxide at clinically achievable concentrations. *J Natl Cancer Inst* 1999; 91: 772–778.
27. Huang Y, Du KM, Xue ZH, et al. Cobalt chloride and low oxygen tension trigger differentiation of acute myeloid leukemic cells: possible mediation of hypoxia-inducible factor-1 $\alpha$ . *Leukemia* 2003; 17: 2065–2073.
28. Jiang Y, Shen WJ, Xue ZH, et al. Desferrioxamine induces leukemic cell differentiation by hypoxia inducible factor-1 $\alpha$  and CCAAT/enhancer-binding protein-a-dependent mechanisms. *Leukemia* 2005; 19: 1239–1247.
29. Overbeeke R, Steffens-Nakken H, Vermes I, Reutelingsperger C, Haanen C. Early features of apoptosis detected by four different flow cytometry assays. *Apoptosis* 1998; 3: 115–121.

30. Chen GQ, Zhu J, Shi XG, *et al.* In vitro studies on cellular and molecular mechanisms of arsenic trioxide (As<sub>2</sub>O<sub>3</sub>) in the treatment of acute promyelocytic leukemia: As<sub>2</sub>O<sub>3</sub> induces NB4 cell apoptosis with downregulation of Bcl-2 expression and alteration of PML-RAR/PML protein localization. *Blood* 1996; **88**: 1052–1061.
31. Debatin KM. Apoptosis pathways in cancer and cancer therapy. *Cancer Immunol Immunother* 2004; **53**: 153–159.
32. Muzio M, Chinnaiyan AM, Kischkel FC, *et al.* FLICE, a novel FADD-homologous ICE/CED-3-like protease, is recruited to the CD95 (Fas/APO-1) death-inducing signaling complex. *Cell* 1996; **85**: 817–827.
33. Gao N, Ding M, Zheng JZ, *et al.* Vanadate-induced expression of hypoxia-inducible factor 1 alpha and vascular endothelial growth factor through phosphatidylinositol 3-kinase/Akt pathway and reactive oxygen species. *J Biol Chem* 2002; **277**: 31963–31971.
34. Papapetropoulos A, Fulton D, Lin MI, *et al.* Vanadate is a potent activator of endothelial nitric-oxide synthase: evidence for the role of the serine/threonine kinase Akt and the 90-kDa heat shock protein. *Mol Pharmacol* 2004; **65**: 407–415.
35. Weinberg ED. The role of iron in cancer. *Eur J Cancer Prev* 1996; **5**: 19–36.
36. Hsing AW, McLaughlin JK, Olsen JH, Mellekjær L, Wacholder S, Fraumeni JF Jr. Cancer risk following primary hemochromatosis: a population-based cohort study in Denmark. *Int J Cancer* 1995; **60**: 160–162.
37. Stevens RG, Graubard BI, Micozzi MS, Neriishi K, Blumberg BS. Moderate elevation of body iron level and increased risk of cancer occurrence and death. *Int J Cancer* 1994; **56**: 364–369.
38. Lovejoy DB, Richardson DR. Iron chelators as anti-neoplastic agents: current developments and promise of the PIH class of chelators. *Curr Med Chem* 2003; **10**: 1035–1049.
39. Tam TF, Leung-Toung R, Li W, Wang Y, Karimian K, Spino M. Iron chelator research: past, present, and future. *Curr Med Chem* 2003; **10**: 983–995.
40. Chan DA, Sutphin PD, Denko NC, Giaccia AJ. Role of prolyl hydroxylation in oncogenically stabilized hypoxia-inducible factor-1alpha. *J Biol Chem* 2002; **277**: 40112–40117.
41. Weng C, Li Y, Xu D, Shi Y, Tang H. Specific Cleavage of Mcl-1 by Caspase-3 in tumor necrosis factor-related apoptosis-inducing ligand (TRAIL)-induced apoptosis in Jurkat leukemia T cells. *J Biol Chem* 2005; **280**: 10491–10500.
42. Minet E, Michel G, Rémacle J, Michiels C. Role of HIF-1 as a transcription factor involved in embryonic development, cancer progression and apoptosis. *Int J Mol Med* 2000; **5**: 253–259.
43. Semenza GL. Hypoxia-inducible factor 1: oxygen homeostasis and disease pathophysiology. *Trends Mol Med* 2001; **7**: 345–350.
44. Greijer AE, van der Wall E. The role of hypoxia inducible factor 1 (HIF-1) in hypoxia induced apoptosis. *J Clin Pathol* 2004; **57**: 1009–1014.
45. Piret JP, Mottet D, Raes M, Michiels C. Is HIF-1alpha a pro- or an anti-apoptotic protein? *Biochem Pharmacol* 2002; **64**: 889–892.
46. Xue ZH, Jiang Y, Yu Y, Wang LS, Chen GQ, Zhao Q. Metavanadate suppresses desferrioxamine-induced leukemic cell differentiation with reduced hypoxia inducible factor-1alpha protein. *Biochem Biophys Res Commun* 2005; **332**: 1140–1147.
47. Haendeler J, Zeiher AM, Dimmeler S. Nitric oxide and apoptosis. *Vitam Horm* 1999; **57**: 49–77.
48. Levenon AL, Patel RP, Brookes P, *et al.* Mechanisms of cell signaling by nitric oxide and peroxynitrite: from mitochondria to MAP kinases. *Antioxid Redox Signal* 2001; **3**: 215–229.
49. Kotamraju S, Tampo Y, Kalivendi SV, Joseph J, Chitambar CR, Kalyanaraman B. Nitric oxide mitigates peroxide-induced iron-signaling, oxidative damage, and apoptosis in endothelial cells: role of proteasomal function? *Arch Biochem Biophys* 2004; **423**: 74–80.
50. Gumprich E, Dahl R, Yerushalmi B, Devereaux MW, Sokol RJ. Nitric oxide ameliorates hydrophobic bile acid-induced apoptosis in isolated rat hepatocytes by non-mitochondrial pathways. *J Biol Chem* 2002; **277**: 25823–25830.
51. Maejima Y, Adachi S, Ito H, Nobori K, Tamamori-Adachi M, Isobe M. Nitric oxide inhibits ischemia/reperfusion-induced myocardial apoptosis by modulating cyclin A-associated kinase activity. *Cardiovasc Res* 2003; **59**: 308–320.